AoI and Throughput Tradeoffs in Routing-aware Multi-hop Wireless Networks

Jiadong Lou*, Xu Yuan*, Sastry Kompella†, and Nian-Feng Tzeng*
*University of Louisiana at Lafayette, Lafayette, Louisiana, USA
†U.S. Naval Research Laboratory, Washington D.C., USA

***Abstract*—The Age-of-Information (AoI) is a newly introduced metric for capturing information updating timeliness, as opposed to the network throughput, which is a conventional performance metric to measure the network transmission speed and robustness as a whole. While considerable work has addressed either optimal AoI or throughput individually, the inherent relationships between the two performance metrics are yet to be explored, especially in multi-hop networks. In this paper, we explore their relationships in multi-hop networks for the very first time, particularly focusing on the impacts of flexible routes on the two metrics. By developing a rigorous mathematical model with interference, channel allocation, link scheduling, and routing path selection taken into consideration, we build the interrelation between AoI and throughput in multi-hop networks. A multi-criteria optimization problem is formulated with the goal of simultaneously minimizing AoI and maximizing network throughput. To solve this problem, we resort to a novel approach by transforming the multi-criteria problem into a single objective one so as to find the weakly Pareto-optimal points iteratively, thereby allowing us to screen all Pareto-optimal points for the solution. A new algorithm based on the piecewise linearization technique is then developed to closely linearize the non-linear terms in the single objective problem via their linear approximation segments to make it solvable. We formally prove that our algorithms can find all Pareto-optimal points in a finite number of iterations. From simulation results, we identify the tradeoff points of the optimal AoI and throughput, demonstrating that one performance metric improves at the expense of degrading the other, with the routing path found as one of the key factors in determining such a tradeoff.**

I. Introduction

Timely updates are deemed absolutely essential in nowadays emerging applications in Cyber-Physical Systems (CPS) and Internet of Things (IoT), critically important for punctual responses. The Age-of-Information (AoI) [1], [2] is a new emerging performance metric proposed to better measure such information updates timeliness. Defined as the time elapsed since the generation time of the latest arrival packet at a target node, AoI characterizes timely information delivery at the destination. In contrast to the conventional metrics of delay and throughput, which capture the effectiveness of data collection and transmission for the overall networks (e.g., delay reflects the mean transmission time of all packets), AoI aims to quantify the time-critical updates at a receiver. Specifically, the optimal AoI has been demonstrated in [2] to be significantly different from the minimized delay.

For correspondence, please contact Prof. Xu Yuan (xu.yuan@louisiana.edu).

Although AoI has its prominent advantage on characterizing information freshness, the throughput metric, which gauges the network transmission speed and robustness, cannot be ignored. For instance, in a large-scale smart home network, plenty of various smart devices are deployed to gather monitoring information. In such a network, high throughput is a necessary requirement to handle massive data uploads, while the lower AoI is also crucial to meet the timely response for urgent events. An immediate question arises here: Once AoI is optimized at the receiver, will the network throughput be boosted or hindered, especially in multi-hop wireless networks?

To date, AoI research have focused extensively on single-hop networks. Efforts have been put in pursuit of AoI optimization by considering packet generation control [1], [2], [3], various queue management mechanisms [4], [5], [6], and scheduling policies [7], [8], [9], [10]. Moreover, the multi-access techniques, including ALOHA and Round Robbin, are considered in [11], [12] to bring AoI into realistic network settings. Meanwhile, different network environments (e.g., with constraints on interference [13], throughput [14], and energy [15]) have been studied for AoI optimization under certain constraints. However, the relationship of AoI and throughput has never been explored in any prior work. While [14] has considered the throughput constraint in its exploitation on AoI optimization, the relationship between AoI and throughput is unexplored therein. In [16], authors discuss the relationship between throughput and AoI optimization in the single-hop network without systematical analysis.

The study of AoI in multi-hop networks is rarely attempted although it has gained increasing interests in the ad-hoc network systems, such as smart cities, vehicular communications, weather forecasting, among others, where emerging applications are urgent while the deployment of sensors or monitors are scattered across a broad area that is far away from the control center. Prior AoI studies on multi-hop networks limit their scopes to either a special network topology or an abstracted network setting. For example, [17] dealt with AoI in the gossip network, while [18] considered a two-hop network for AoI optimization. In [19], AoI for multi-hop networks with general interference constraints was pursued, but its analytic models simplify the network setting by pre-grouping interference-free sets without taking into account the channel allocation. All existing work on multi-hop networks fails to take into consideration, such realistic factors as channel access modulation and routing, and to pursue the AoI and

throughput relationships.

In this paper, we study AoI and throughput optimization in routing-aware multi-hop networks for the first time, aiming to explore the inherent relationships between AoI and throughput. The network is assumed to employ OFDM channel access modulation, with scheduling and link activation based on the orthogonal channels. As a source may have multiple potential paths to route its packets to a given destination node in multi-hop networks, we consider the flexible routing paths selection for sessions while exploring their impacts on the overall AoI and throughput relationship. By characterizing the channel allocation, link scheduling, packet generation, and routes selection, we develop a rigorous model for relating AoI to throughput in multi-hop networks. With the developed model, we formulate a multi-criteria optimization problem with the objectives of simultaneously minimizing AoI and maximizing throughput.

As the developed multi-criteria problem is in the complex form of non-linear and non-convex programming, we develop a novel algorithm to solve it efficiently, with an aim at determining all AoI and throughput tradeoff points, i.e., Pareto-optimal points. The proposed algorithm first transforms the multi-criteria problem into a single objective one, so as to find the weakly Pareto-optimal points iteratively and then to screen Pareto-optimal points for the solution. Since the transformed single objective problem is in the non-linear form, we design another algorithm based on the piece-wise linearization technique to reformulate the non-linear terms approximately into a set of linear segments so that such a single objective problem is solvable by commercial software efficiently. It is formally proved that the proposed algorithm can find all Pareto-optimal points in a finite number of iterations. The significance of finding all Pareto-optimal points is that it offers the entire landscape of achievable throughput and AoI tradeoffs, which provides us the global view of the relationships between them. In contrast, a solution to the traditional problem such as maximizing throughput under AoI constraints or minimizing AoI under throughput constraints only represents one point in our solutions. Moreover, under certain scenarios where one performance metric (AoI or throughput) has a higher priority than the other one, the network operator can always find an optimal tradeoff between AoI and throughput instantly from the set of our Pareto-optimal points.

We conduct the simulation evaluation to quantify AoI and throughput performance with the flexible routes. The global landscape of AoI and throughput relationships is presented, demonstrating that the improvement in one metric is at the expense of deteriorating the other metric, with the routing path identified as one of the key factors in dictating such a tradeoff between optimal AoI and throughput.

The remainder of this paper is organized as follows. Section II presents the mathematical model and multi-criteria problem formulation for AoI and throughput optimization. In Section III, we develop a novel algorithm to solve the multi-criteria problem with the aim to find all AoI and throughput tradeoff points. In Section IV, we develop an algorithm based on the piece-wise linearization technique to transform nonlinear terms in the derived single objective problem (given in Section III) into a set of linear segments to make it solvable. Section V presents numerical results and Section VI concludes this paper.

II. Mathematical Modeling and Formulation

We consider a multi-hop wireless network comprising of a set of nodes $\mathcal{N}$. Suppose all nodes employ the OFDM channel access modulation for data transmission and a set of $\mathcal{B}$ orthogonal channels (with equal bandwidth) exists for scheduling. There is a set of sessions $\mathcal{L}$ in this network, where the source and destination nodes of each session $l \in \mathcal{L}$ are denoted as s_l and d_l, respectively. The routes from source to destination nodes of all sessions are not pre-fixed, and each session has the flexibility to select the appropriate route so as to meet its transmission needs. Each session involves the time-sensitive applications, calling for freshness information updates from its source to the destination timely. We take the *Age of Information (AoI)* as the metric of choice to measure the information updating timeliness. On the other hand, the network throughput which gauges the packet transmission speed and robustness is also an important criterion that should be taken into consideration. The goal of this paper is to explore the interrelation of AoI and network throughput in OFDM-based multi-hop wireless networks.

A. Network Model

Let $\mathcal{T}_i$ denote the set of nodes in $\mathcal{N}$ located within node i's transmission range. Since the route for each session is not pre-fixed, i may choose any node in its transmission range to receive its transmitted data. We let a binary variable $n_{ij}^l[b]$ indicate if a link (i,j) is set up (i.e., activated) in a channel b for a session l as follows:

$$n_{ij}^l[b] = \begin{cases} 1, & \text{if the link } (i,j) \text{ is activated in channel } b \\ & \text{for sesssion } l, \\ 0, & \text{otherwise.} \end{cases} \tag{1}$$

where $i \in \mathcal{N}, j \in \mathcal{T}_i, l \in \mathcal{L}, b \in \mathcal{B}$.

Assume that all sessions are unicast, i.e., node i can receive from or transmit to only one node in a channel, we have:

$$\sum_{l\in\mathcal{L}} \sum_{j\in\mathcal{T}_i} n_{ij}^l[b] \leq 1 \ , \ (i \in \mathcal{N}, b \in \mathcal{B}) \ . \tag{2}$$

$$\sum_{l\in\mathcal{L}} \sum_{k\in\mathcal{T}_i} n_{ki}^l[b] \leq 1 \ , \ (i \in \mathcal{N}, b \in \mathcal{B}) \ . \tag{3}$$

To account for half-duplex at each node, we have:

$$\sum_{l\in\mathcal{L}} n_{ij}^l[b] + \sum_{l\in\mathcal{L}} n_{ki}^l[b] \leq 1 \ , \ (i \in \mathcal{N}, j,k \in \mathcal{T}_i, b \in \mathcal{B}) \ . \tag{4}$$

The above unicast and half-duplex constraints (2) (3), and (4) can be replaced equivalently by the following constraint:

$$\sum_{l\in\mathcal{L}} \sum_{j\in\mathcal{T}_i} n_{ij}^l[b] + \sum_{l\in\mathcal{L}} \sum_{k\in\mathcal{T}_i} n_{ki}^l[b] \leq 1 \ , \ (i \in \mathcal{N}, b \in \mathcal{B}) \ . \tag{5}$$

To model interference among activated links, we denote $\mathcal{I}_i$ as the set of nodes located within the interference range of a node $i \in \mathcal{N}$. Then, we have:

$$\sum_{l\in\mathcal{L}} n_{ij}^l[b] + \sum_{l\in\mathcal{L}} n_{ph}^l[b] \leq 1 \ , \tag{6}$$

where $i \in \mathcal{T}_j, p \in \mathcal{I}_j, h \in \mathcal{T}_p, j \in \mathcal{N}, j \neq h$, and $b \in \mathcal{B}$. This means if a node j is receiving on channel b, it will not be interfered on the same channel by an unintended transmitter p that locates within j's interference range.

Link Activation Frequency. Let f_{ij}^l denotes the activation frequency of a link (i, j) among all channels for a session l, we have:

$$f_{ij}^l = \sum_{b\in\mathcal{B}} n_{ij}^l[b] \ , (i \in \mathcal{N}, l \in \mathcal{L}, j \in \mathcal{T}_i) \ . \tag{7}$$

Let binary variable z_{ij}^l represent if a link (i, j) is set up for session l, it deified as follows:

$$z_{ij}^l = \begin{cases} 1, & \text{if } f_{ij}^l \geq 1, \\ 0, & \text{otherwise.} \end{cases} \tag{8}$$

This means if a link (i, j) is set up only if the activation frequency of this link for session l is no less than 1. This statement can be reformulated mathematically into the following forms:

$$f_{ij}^l \geq z_{ij}^l \ , (1 - z_{ij}^l) f_{ij}^l < 1 \ . \tag{9}$$

Routing Constraints. Each session needs to find its route to carry packets from its source to the destination. Suppose there is only one path for each session and the paths from different sessions can intersect at some nodes but no multiple paths share the same link. The routing path for each session $l \in \mathcal{L}$ can be formulated as follows.

- If node i is the source of a session l, we have:

$$\sum_{j\in\mathcal{T}_i} z_{ij}^l = 1 \ , \ (i = s_l). \tag{10}$$

- If node i is an intermediate node for a session l, we have:

$$\sum_{j\in\mathcal{T}_i, j\neq s_l} z_{ij}^l = \sum_{k\in\mathcal{T}_i, k\neq d_l} z_{ki}^l \ , \ (i \neq s_l, i \neq d_l). \tag{11}$$

- If node i is the destination node of a session l, we have:

$$\sum_{k\in T_i} z_{ki}^l = 1 \ , \ (i = d_l). \tag{12}$$

Since no link is shared by multiple sessions, we define two other variables f_{ij} and z_{ij} as $f_{ij} = \sum_{l\in\mathcal{L}} f_{ij}^l$ and $z_{ij} = \sum_{l\in\mathcal{L}} z_{ij}^l$. We have:

$$z_{ij} \leq 1 \ , \ (i \in \mathcal{N}, j \in \mathcal{T}_i) \ . \tag{13}$$

Packet Transmission Model. Assuming that senders in all sessions are always working to produce updates, and they divide or adapt the generated data into packets of a uniform size for transmission, denoted as d. Denote λ^l as the generation rate at source s_l of session l. Then, the time interval of packet generation at the sender s_l is the constant $\frac{1}{\lambda^l}$. Let μ_{ij} denote the transmission rate of link (i, j), with the rate constrained by the total link capacity. We have:

$$\mu_{ij} \leq f_{ij} C_{ij} \ , \tag{14}$$

where f_{ij} is the link activation frequency of all sessions. Here, C_{ij} accounts for the link capacity in a link (i, j), we have:

$$C_{ij} = W_B \log_2(1 + \frac{p_i d_{ij}^{-\gamma} \delta}{N_0}) \ , \tag{15}$$

where W_B being the bandwidth of each channel b, p_i the power spectral density from transmit node i, d_{ij} the distance between nodes i and j, γ the path loss index, δ the antenna-related constant, and N_0 the ambient Gaussian noise density.

When the network reaches the steady-state, to avoid the packet loss caused by the infinite number of backlogged packets at any relay node, the transmission time of each packet on a link should be no larger than the packet generation time interval of the session that employs it. Hence, we have $\frac{1}{\lambda^l} \geq \frac{d}{\mu_{ij}}$ for each activated link. Since no link is shared with multiple sessions, this can be reformulated as follows:

$$\mu_{ij} \geq \sum_{l\in\mathcal{L}} \lambda^l d z_{ij}^l \ . \tag{16}$$

Throughput Model. All packets are assumed to be always delivered successfully to destination nodes. Within a time range $(0, T)$, the throughput of session l (denoted as U^l) can be expressed as

$$U^l = \frac{Kd}{T} = \lambda^l d \ , \tag{17}$$

where K is the total number of packets generated within $(0, T)$ for this session. Hence, the constraint (16) can be rewritten as:

$$\mu_{ij} \geq \sum_{l\in\mathcal{L}} U^l z_{ij}^l \ . \tag{18}$$

B. AoI Model

Let $D_{d_l}(t)$ indicate the generation time of the latest packet reaching the destination node $d_l, l \in \mathcal{L}$. The instantaneous AoI at time t, denoted by $a_{d_l}(t)$, is calculated by $a_{d_l}(t) = t - D_{d_l}(t)$. Based on the graphical argument, the total aggregated AoI, denoted as ΔA_{d_l}, over time range $(0, T)$ at a destination node d_l can be calculated by the area under the curve of instantaneous AoI, i.e.,

$$\Delta A_{d_l} = \int_0^T a_{d_l}(t) dt \ . \tag{19}$$

Then, the time averaged AoI at the destination node d_l (denoted as A_{d_l}) in time range $(0, T)$ is expressed by:

$$A_{d_l} = \frac{1}{T} \int_0^T a_{d_l}(t) dt \ . \tag{20}$$

To model AoI in the multi-hop networks, we first find the AoI relationships of two consecutive nodes and then derive AoI at a destination node recursively. Let A_i^l and A_j^l denote the time averaged AoI at a node i and its successor node j for the packets from a session $l \in \mathcal{L}$. We have:

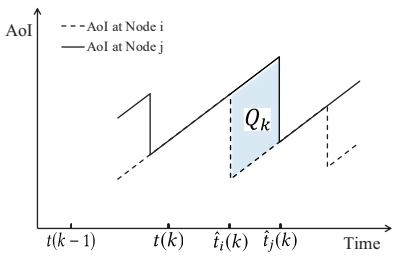

Fig. 1. AoI variation at two consecutive nodes.

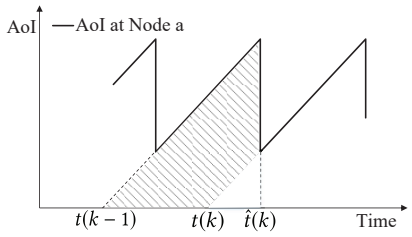

Fig. 2. AoI variation at node a, the successor of source node s_l.

Lemma 1. *If a link (i,j) is set up between node i and node j, time averaged AoIs for packets (from the same source node s_l) at these two nodes satisfy the following relationship:*

$$A_j^l = A_i^l + \frac{d}{\mu_{ij}} \ . \tag{21}$$

Proof. The proof is based on the graphical approach. As shown in Figure 1, the kth packet is generated at time $t(k)$ and reaches node i and node j at time $\hat{t}_i(k)$ and $\hat{t}_j(k)$, respectively. Assume a packet arriving at a node can be transmitted to its successor node immediately without considering the propagation delay. Here, the dashed and solid lines represent the AoI at nodes i and j, respectively. The difference of the aggregated AoIs at nodes i and j during time $(0,T)$ equals the sum of shadow parallelogram parts labeled in Figure 1. We have:

$$\Delta A_j^l = \Delta A_i^l + \sum_{k=1}^{K} Q_k \ , \tag{22}$$

where K is the number of packets delivered within the time span of $(0,T)$ and Q_k is the area of kth parallelogram. From Figure 1, the area Q_k is expressed as the product of $\hat{t}_j(k) - \hat{t}_i(k)$ and $t(k) - t(k-1)$, which are the transmission time of a packet via link (i,j) and the packet generation interval, respectively. Hence, (22) can be given by

$$\Delta A_j^l = \Delta A_i^l + \sum_{k=1}^{K} \frac{1}{\lambda^l}\frac{d}{\mu_{ij}} \ . \tag{23}$$

Then, we have the time averaged AoI at node j within $(0,T)$ as follows:

$$\begin{aligned} A_j^l &= \frac{\Delta A_i^l + \sum_{k=1}^{K} \frac{1}{\lambda^l}\frac{d}{\mu_{ij}}}{T} = A_i^l + \frac{K}{T}\frac{\sum_{k=1}^{K} \frac{1}{\lambda^l}\frac{d}{\mu_{ij}}}{K} \\ &= A_i^l + \frac{d}{\mu_{ij}} \ , \end{aligned} \tag{24}$$

where the term $\frac{K}{T}$ is equal to the packet generation rate λ^l. □

The importance of Lemma 1 is that it enables us to recursively derive the time averaged AoI at a destination node d_l iteratively starting from the source node s_l. Besides, Lemma 1 also indicates that the increase in AoI through the session mainly due to the delay introduced in the multi-hop transmission.

Theorem 1. *Time averaged AoI at the destination node $d_l, l \in \mathcal{L}$, can be calculated by:*

$$A_{d_l} = \frac{1}{2\lambda^l} + \sum_{i \neq d_l, z_{ij}^l = 1} \frac{d}{\mu_{ij}} \ , \tag{25}$$

where j is i's successor node and $z_{ij}^l = 1$ represents that link (i,j) is set up for transmitting packets over session l.

Proof. Based on Lemma 1, time averaged AoI at the destination node d_l can be calculated iteratively from the source node s_l's successor node a (where $z_{s_l a}^l = 1$). Hence, we have:

$$A_{d_l} = A_a^l + \sum_{i \neq d_l, i \neq s_l, z_{ij}^l = 1} \frac{d}{\mu_{ij}} \ . \tag{26}$$

Here, $z_{ij}^l = 1$ represents that link (i,j) is set up for transmitting packets over session l. From Figure 2, the aggregated AoI at the node a for session l, denoted by ΔA_a^l, equals the sum of trapezoid parts, accounting the area difference between two isosceles right triangles. Hence, we have:

$$\Delta A_a^l = \sum_{k=1}^{K} \{ \frac{1}{2}[\hat{t}(k) - t(k-1)]^2 - \frac{1}{2}[\hat{t}(k) - t(k)]^2 \} \ , \tag{27}$$

where K is the number of packets delivered to node a. In Figure 2, the kth packet is generated at time $t(k)$ and received by node a at $\hat{t}(k)$. The term of $t(k) - t(k-1)$ is the time interval of packets generation, which equals $\frac{1}{\lambda^l}$, and the term $\hat{t}(k) - t(k)$ is the packet transmission time, which equals $\frac{d}{\mu_{s_l a}}$. As a result, the aggregated AoI can be calculated by:

$$\begin{aligned} \Delta A_a^l &= \sum_{k=1}^{K} \{ \frac{1}{2}[\hat{t}(k) - t(k-1)]^2 - \frac{1}{2}[\hat{t}(k) - t(k)]^2 \} \\ &= \sum_{k=1}^{K} [\frac{1}{2}(\frac{1}{\lambda^l} + \frac{d}{\mu_{s_l a}})^2 - \frac{1}{2}(\frac{d}{\mu_{s_l a}})^2] \\ &= \sum_{k=1}^{K} (\frac{1}{2\lambda^{l^2}} + \frac{d}{\lambda^l \mu_{s_l a}}) \ . \end{aligned} \tag{28}$$

Thus, time averaged AoI at node a over $(0, T)$ is:

$$A_a^l = \frac{\sum_{k=1}^{K}(\frac{1}{2\lambda^{l2}} + \frac{d}{\lambda^l \mu_{s_l a}})}{T} = \frac{K}{T}\frac{\sum_{k=1}^{K}(\frac{1}{2\lambda^{l2}} + \frac{d}{\lambda^l \mu_{s_l a}})}{K} = \lambda^l(\frac{1}{2\lambda^{l2}} + \frac{d}{\lambda^l \mu_{s_l a}}) = \frac{1}{2\lambda^l} + \frac{d}{\mu_{s_l a}} \ . \quad (29)$$

Combining (29) and (26), we have:

$$A_{d_l} = A_a + \sum_{i \neq d_l, i \neq s_l}^{z_{ij}^l=1} \frac{d}{\mu_{ij}} = \frac{1}{2\lambda^l} + \frac{d}{\mu_{s_l a}} + \sum_{i \neq d_l, i \neq s_l}^{z_{ij}^l=1} \frac{d}{\mu_{ij}} = \frac{1}{2\lambda^l} + \sum_{i \neq d_l, z_{ij}^l=1} \frac{d}{\mu_{ij}} \ .$$

□

From (25), we notice that the first term is related to packet generation interval while the second term comes from the transmission delay over the multiple traversed links on the specified session route. Such an AoI formula indicates that the minimization of AoI is a comprehensive work involving the generation rate control, routing selection scheme, and the delay management together.

Denote A^{ave} as the time averaged AoI of all sessions, then

$$A_{ave} = \sum_{l \in \mathcal{L}} A_{d_l} = \sum_{l \in \mathcal{L}} (\frac{1}{2\lambda^l} + \sum_{i \neq d_l, z_{ij}^l=1} \frac{d}{\mu_{ij}}) = \sum_{l \in \mathcal{L}} \frac{1}{2\lambda^l} + \sum_{i \in \mathcal{N}} \sum_{j \in \mathcal{T}_i, z_{ij}^l=1} \frac{d}{\mu_{ij}} \ . \quad (30)$$

C. Problem Formulation

With our developed model, we aim to maximize throughput and minimize AoI. For throughput, we are interested in maximizing the minimum throughput (denoted as $U_{\min}$) among all sessions, i.e.,

$$U_{\min} \leq U^l, l \in \mathcal{L} \ . \quad (31)$$

Our problem can be formulated as a multi-criteria optimization problem with the objectives of minimizing AoI and maximizing throughput across all sessions. That is,

$$\begin{aligned} \text{OPT} \quad & \min A_{ave} \\ & \max U_{\min} \\ & s.t. \text{ The total time averaged AoI function: } (30); \\ & \quad \text{Interference constraints: } (5),\ (6); \\ & \quad \text{Links activation frequency: } (9); \\ & \quad \text{Routing constraints: } (10),\ (11),\ (12),\ (13); \\ & \quad \text{Transmission model: } (14),\ (18); \\ & \quad \text{Throughput model: } (17),\ (31). \end{aligned}$$

From OPT, we observe that the solution for the optimal throughput may not lead to the minimal achievable AoI value as each of them wishes to find the best resource allocation and routing solutions for optimality individually. Improving one objective may deteriorate the other one, and thus the two objectives of throughput and AoI may conflict with each other, which will also be demonstrated by our simulation results given in Section V. The next section develops an efficient solution for this multi-criteria optimization problem.

III. Algorithm Design for AoI and Throughput Tradeoffs

In OPT, we aim to simultaneously minimize AoI and maximize throughput by pursuing the *Pareto-optimal points* to exhibit their tradeoffs. The goal of our design is to develop an algorithm that finds all Pareto-optimal points, corresponding to all optimal values, for the multi-objective problem OPT.

A. Background for Pareto-optimal Solution

A Pareto-optimal point is a state of resources allocation where neither objective can be improved without deteriorating the other. The solution corresponding to a Pareto-optimal point is called the *Pareto-optimal solution*. For a Pareto-optimal solution ϕ^*, if the objective pair $(A_{ave}^*, U_{\min}^*)$ is *a Pareto-optimal point*, there is no other feasible solution ϕ with the objective pair $(A_{ave}, U_{\min})$ such that $A_{ave} < A_{ave}^*$ and $U_{min} \geq U_{\min}^*$, or $A_{ave} \leq A_{ave}^*$ and $U_{\min} > U_{\min}^*$. This means it is impossible to find another solution to make AoI lower without degrading throughput, or to increase throughput without deteriorating AoI. Besides, an objective pair $(\tilde{A}_{ave}, \tilde{U}_{\min})$ to the solution $\tilde{\phi}$ is a *weakly Pareto-optimal point* if there does not exist a solution ϕ with $A_{ave} < \tilde{A}_{ave}$ and $U_{\min} > \tilde{U}_{\min}$. It is apparent that a Pareto-optimal point is also a weakly Pareto-optimal point whereas a weakly Pareto-optimal point is not always a Pareto-optimal point.

B. Relationships between Two Metrics

Based on (17) and (30), we have:

$$A_{ave} = \sum_{l \in \mathcal{L}} \frac{1}{2\lambda^l} + \sum_{i \in \mathcal{N}} \sum_{j \in \mathcal{T}_i}^{z_{ij}=1} \frac{d}{\mu_{ij}} = \sum_{l \in \mathcal{L}} \frac{d}{2U^l} + \sum_{i \in \mathcal{N}} \sum_{j \in \mathcal{T}_i}^{z_{ij}=1} \frac{d}{\mu_{ij}} \ . \quad (32)$$

Let $\mathcal{H}(\mathbf{R}, \mathbf{U}) = A_{ave}$ and $\mathbf{R} = \{\mathbf{n}, \mathbf{f}, \mathbf{z}\}$ represent resource allocation solutions where $\mathbf{U} = \{U^l | l \in \mathcal{L}\}$. For a given route and one resource allocation of session l, we have:

$$\frac{\partial \mathcal{H}}{\partial U^l} = -\frac{d}{2U^{l2}} \leq 0 \ , \quad (33)$$

This indicates that AoI minimized as throughput increases with determined routing and given channel allocation solutions. However, based on constraints (18) and (14), the throughput with a fixed route is limited to the bottleneck link capacity and the avoidance of the unbound delay caused by infinite queuing

at some relay nodes. Let U_R denote the maximum throughput achievable under certain solution $\mathbf{R}$. We have:

$$U_R = \min_{z_{ij}=1} \{f_{ij} C_{ij}\} \ , \tag{34}$$

where the variable z of every link in the fixed route is 1. For a given routing solution $\mathbf{R}$, once AoI achieves its minimum value, throughput is limited to the value of U_R.

C. Finding a Weakly Pareto-Optimal Point

In this section, we provide a two-step approach for determining a weakly Pareto-optimal point. First, we reformulate OPT into a single AoI objective problem by adding a new throughput constraint v while removing the throughput objective function. This problem is reformulated as follows:

OPT-AoI

$\min \ A_{ave}$

$s.t.$ Throughput constraint: $U_{\min} > v$;

Constraints: $(5), (6), (9) - (14), (17), (18), (30), (31)$.

By solving this problem, we get an optimal AoI value (denoted as A^v_{ave}) with a routing solution (denoted as $\mathbf{R}^v$). Notably, OPT-AoI is in the form of mixed-integer nonlinear programming, which cannot be solved directly. Our developed linearized algorithm (elaborated in Section IV) is applied here to linearize the non-linear terms in the objective function into a set of linear segments to make OPT-AoI solvable by commercial solvers. Second, we find the maximum throughput under solution $\mathbf{R}^v$ by (34), denoted as U_{R^v}.

Lemma 2. *The objective pair (A^v_{ave}, U_{R^v}) is a weakly Pareto-optimal point.*

Proof. The proof is based on contradiction. Assume that the pair (A^v_{ave}, U_{R^v}) is not a weakly Pareto-optimal point. There must be a solution $\phi^{'}$ with an objective pair $(A^{v^{'}}_{ave}, U^{'}_{R^v})$, that satisfies $A^{v^{'}}_{ave} < A^v_{ave}$ and $U^{'}_{R^v} > U_{R^v}$. Since $U^{'}_{R^v} > U_{R^v} > v$, $\phi^{'}$ is a feasible solution to problem OPT-AoI. However, given A^v_{ave} is the minimum value in this problem, we have $A^{v^{'}}_{ave} \geq A^v_{ave}$, contradicting the assumption. □

Since a Pareto-optimal point is also a weakly Pareto-optimal point, if we find all weakly Pareto-optimal points, all Pareto-optimal points are then be included.

D. Determining All Pareto-optimal Points

This subsection provides an algorithm to determine all Pareto-optimal points. While Section III-C describes how to find a weakly Pareto-optimal point with a constant v, there are an infinite number of values for v, making it impractical to traverse all v values to identify all weakly Pareto-optimal points. We provide an effective approach for selecting some v values simply based on those weakly Pareto-optimal points found, instead of arbitrarily searching for all v values. The essence of our algorithm is to jump the routing path from one to another by adjusting the values of v, with the following general idea. In each iteration, an OPT-AoI problem is solved with a throughput constraint v to find an optimal value of AoI. The maximum throughput can be calculated based on the current solution. Hence, we get a weakly Pareto-optimal pair and then set v as the current maximum throughput value for the next iteration. By comparing the AoI values, we single out all Pareto-optimal points among those weakly Pareto-optimal points found. Algorithm details are shown in Algorithm 1.

Algorithm 1 Finding Pareto-optimal Points

Step 1:
Initialization: $v = 0, M = 0, P = (0, 0)$, an empty set $\mathcal{O}$.
Solve OPT-AoI with the parameter v.
Step 2:
while Existing feasible solution to OPT-AoI with the parameter v. **do**
  Step 2.1:
  Record the objective value A^v_{ave} and the routing R^v.
  Calculate U_{R^v} based on (34).
  Add the point $P = (A^v_{ave}, U_{R^v})$ to $\mathcal{O}$.
  Step 2.2:
  if $A^v_{ave} = M$ **then**
    Remove the point P from $\mathcal{O}$.
  end if
  Step 2.3:
  $M = A^v_{ave}$ and $v = U_{R^v}$.
  Solve OPT-AoI with the parameter v.
end while

Theorem 2. *The set $\mathcal{O}$ from Algorithm 1 includes all Pareto-optimal points and the algorithm terminates in a finite number of iterations.*

Proof. The proof consists of three steps. We first show that each objective pair in $\mathcal{O}$ is a Pareto-optimal point. Based on Lemma 2, each objective pair (A^v_{ave}, U_{R^v}) is a weakly Pareto-Optimal point. **Step 2.2** in Algorithm 1 is the screening procedure of Pareto-optimal points among the weakly Pareto-optimal points. Consider two objective pairs, denoted respectively by (A^a_{ave}, U_{R^a}) and (A^b_{ave}, U_{R^b}), and suppose the pair (A^b_{ave}, U_{R^b}) is found in the iteration after (A^a_{ave}, U_{R^a}). Since the parameter v is always equal to the throughput found in the last iteration and the throughout keeps increasing, the solution of A^b_{ave} for OPT-AoI is also a feasible solution for A^a_{ave}, yielding $A^a_{ave} \leq A^b_{ave}$. In Algorithm 1, any weakly Pareto-optimal point with the same AoI value as that of the next point is dropped from the set $\mathcal{O}$, so $A^a_{ave} < A^b_{ave}$. As $U_{R^b} > U_{R^a}$ and $A^a_{ave} < A^b_{ave}$, we conclude that any two consecutive points in $\mathcal{O}$ are Pareto-optimal points.

Next, we prove that all Pareto-optimal points are found by Algorithm 1. This has to show that at each iteration, there is no more Pareto-optimal point whose throughput value is bigger than that found in the previous iteration (denoted as (A^p_{ave}, U_{R^p})) and is smaller than that derived in the current iteration (denoted as (A^c_{ave}, U_{R^c})). This is proved by contradiction. Suppose there is a Pareto-optimal point $(A^{'}_{ave}, U^{'})$ satisfying the above assumption, then $U_{R^p} < U^{'} \leq U_{R^c}$.

As $U^{'} \leq U_{R^c}$, the point $(A^{'}_{ave}, U^{'})$ can be a Pareto-optimal point only if $A^{'}_{ave} < A^{c}_{ave}$, giving rise to improved AoI. Based on the assumption of $U_{R^p} < U^{'}$, the objective pair $(A^{'}_{ave}, U^{'})$ is also a feasible solution for problem OPT-AoI with the throughput constraint of $U > U_{R^p}$. Since A^{c}_{ave} is the optimal value under this constraint, we have $A^{'}_{ave} \geq A^{c}_{ave}$. This contradicts to $A^{'}_{ave} < A^{c}_{ave}$. Thus, there is no other Pareto-optimal point existing between two neighboring ones.

Finally, we show that Algorithm 1 terminates in a finite number of iterations. Since the activation frequency is an integer variable in range $(0, |\mathcal{B}|)$ and C_{ij} has at most $\mathcal{N}^2$ different values, based on (34), the numbers of viable U_{R^v} and of v values are at most $|\mathcal{B}| \cdot |\mathcal{N}|^2$. Besides, from the throughput constraint in problem OPT-AoI and **Step 2.3** in Algorithm 1, the value of throughput threshold v increases with each iteration. Hence, Algorithm 1 terminates in a finite number of iterations. □

IV. Linearization of OPT-AoI

The last section outlines a solution for determining all Pareto-optimal points iteratively for the multi-criteria problem of OPT. However, in each iteration, a single objective problem OPT-AoI needs to be solved to find a corresponding weakly Pareto-optimal point. As OPT-AoI is in the form of non-linear non-convex programming, we apply the piece-wise linearization technique to transform the problem of OPT-AoI into mixed-integer linear programming (MILP), so that it can be directly solved by commercial software.

A. Linearization of $\frac{1}{\mu}$

A nonlinear part of OPT-AoI lies in the objective function, i.e., $\frac{1}{\mu_{ij}}$ in (32). With $g(x) = \frac{1}{x}$, the objective function then can be replaced by:

$$A^{ave} = \frac{2}{d} \sum_{l \in \mathcal{L}} \frac{1}{U^l} + d \sum_{i \in \mathcal{N}} \sum_{j \in \mathcal{T}_i}^{z_{ij}=1} g(\mu_{ij}) \ .$$

As $\frac{\partial g(\mu)}{\partial \mu^2} = \frac{2}{\mu^3} > 0$, $g(\mu)$ proved to be a convex function. This allows us to employ the piece-wise linearization technique to approximate the curve of $g(\mu)$ with a set of linear segments while ensuring the gap between the value of any point on $g(\mu)$ and that on the corresponding linear segments to stay within an approximate error η.

We denote the minimum value of μ as $C^{\min}$, which is C_{ij} of the bottleneck link among all sessions. Since the maximum value of f_{ij} is $|\mathcal{B}|$, μ is upper bounded by $|\mathcal{B}|C^{\max}$ (from (14)), where $C^{\max}$ is the maximum value of C_{ij} among all links. Assuming that the minimum number of linear segments is S, μ^0 is the X-axis value for the start point, and $\mu^1, \mu^2 \cdots, \mu^S$ are the X-axis values for the end points of linear segments, we have $\mu^0 = C^{\min}$ and $\mu^S = |\mathcal{B}|C^{\max}$.

To ensure the minimum number of S, we start to calculate the slope of the first segment from μ^0 and ensure the approximate gap between this linear segment and the original curve to be no more than η. With this start point and the slope, we obtain the end point of this segment that intersects with the original curve and treat it as the start point of the second segment, denoted by μ^1. We repeat the above process until finding adequate segments that cover the entire feasible range of μ. Denoting the s-th linear segment and its slope as $G_s(\mu)$ and q^s, respectively, we have:

$$q^s = \frac{g(\mu^s) - g(\mu^{s-1})}{\mu^s - \mu^{s-1}} \ , \tag{35}$$

$$G_s(\mu) = q^s \cdot (\mu - \mu^{s-1}) + g(\mu^{s-1}) \ . \tag{36}$$

Within each range of (μ^{s-1}, μ^s), there is a point with the maximum gap between the linear segment and the curve, denoted as η. If the x-coordinate of that point is denoted by $\hat{\mu}^s$, we have:

$$\frac{\partial g(\hat{\mu}^s)}{\partial \mu} - q^s = 0, \ G_s(\hat{\mu}^s) - g(\hat{\mu}^s) = \eta. \tag{37}$$

The slope q^s can be obtained by solving above equations. If for the start point of the s-th segment with $g(\mu^{s-1}) \leq \eta$, we set its end point at $\mu^s = |\mathcal{B}|C^{max}$ and then have the last segment drawn from $(\mu^{s-1}, g(\mu^{s-1}))$ to $(|\mathcal{B}|C^{max}, g(|\mathcal{B}|C^{max}))$. Algorithm 2 gives the details of finding the values of $\mu^1, \cdots, \mu^S$ and slopes $q^1, \cdots, q^S$ for any given approximate error η,

Algorithm 2 Piece-wise Linearization

Initialization: $s = 1$ and $\mu^{s-1} = C^{min}$.
while $\mu^{s-1} < |\mathcal{B}|C^{max}$ **and** $g(\mu^{s-1}) > \eta$ **do**
  Calculate slop q^s by solving (37).
  With q^s, calculate μ^s based on (35).
  $s = s + 1$.
end while
if $\mu^{s-1} \geq |\mathcal{B}|C^{max}$ **then**
  $S = s - 1, \mu^S = |\mathcal{B}|C^{max}$, and recalculate q^S based on (35).
else if $g(\mu^{s-1}) \leq \eta$ **then**
  $S = s, \mu^S = |\mathcal{B}|C^{max}$, and calculate q^S based on (35).
end if

Lemma 3. *The approximation error within each linear segment derived from Algorithm 2 is no more than η.*

The proof is based on the aforementioned construction process and is omitted here. With Algorithm 2, we can approximate $\frac{1}{\mu}$ in the objective function via a set of linear segments with an error upper bounded by η.

B. Linearization of $\frac{1}{U}$

Similarly, the non-linear part for throughput in the objective function of OPT-AoI also appears in the $g(x)$ form, i.e., $\frac{1}{U^l}$. We follow the same piece-wise linearization solution as above to reformulate it into a set of linear segments with a guaranteed approximate error, denote by η_2. Specifically, it determines the minimum number of linear segments E, the slopes $q^1_u, q^2_u, ..., q^E_u$, the X-axis values $U^0, U^1, U^2 ..., U^E$ of the linear segments. Its detailed discussion is omitted here.

C. Problem Reformulation and Approximate Gap

Let $G(\mu)$ and $G_2(U)$ represent the concatenated linear segments for $\frac{1}{\mu}$ and $\frac{1}{U}$, respectively, derived from Sections IV-A and IV-B. The objective $\min A_{ave}$ of OPT-AoI can be replaced by the following linear function and constraints:

$$\begin{aligned}
\min \quad & A_{ave}^{L} \\
\text{s.t.} \quad & A_{ave}^{L} = \frac{d}{2}\sum_{l\in\mathcal{L}} G_2(U^l) + d\sum_{i\in\mathcal{N}}\sum_{j\in\mathcal{T}_i}^{z_{ij}=1} G(\mu_{ij}) \ ; \qquad (38) \\
& G(\mu_{ij}) \geq q^s\cdot(\mu_{ij}-\mu^{s-1}) + g(\mu^{s-1}) \ , \\
& G_2(U^l) \geq q_u^e\cdot(U^l - U^{e-1}) + g(U^{e-1}) \ , \\
& (s=1,2,\cdots,S, \mu\in[C^{min}, |\mathcal{B}|C^{max}]) \ , \\
& (e=1,2,\cdots,E, U\in[0,|\mathcal{B}|C^{max}]) \ . \qquad (39)
\end{aligned}$$

Then, the original OPT-AoI problem is reformulated into the following new optimization problem, i.e.,

$$\begin{aligned}
\text{OPT-L} \quad & \min A_{ave}^{L} \\
& s.t. \text{ Throughput constraint: } U_{min} > v \ ; \\
& \quad \text{Constraints: } (5),(6),(9)-(14),(17),(18), \\
& \qquad (30),(31),(38),(39).
\end{aligned}$$

OPT-L is in the form of mixed integer linear programming, which can be solved by commercial solvers (e.g., CPLEX) efficiently. The following theorem characterizes the error bound between the optimal objective values of OPT-L and those of the original OPT-AoI problem.

Theorem 3. *The gap between the optimal objective values of OPT-AoI and OPT-L, ϵ, is upper bounded by $\frac{d}{2}\sum_{l\in\mathcal{L}}\eta_2 + d\sum_{i\in\mathcal{N}}\sum_{j\in\mathcal{T}_i}^{z_{ij}=1}\eta$.*

Proof. Suppose the optimal solution of OPT-AoI is $\varphi_{AoI}^{*} = \{n_{ij}^{*}[b], f_{ij}^{*}, z_{ij}^{*}, \mu_{ij}^{*}, U^{l^*}\}$ with the objective value being A_{ave}^{O*}. Because the solution φ_{AoI}^{*} meets all constraints in OPT-L, we can construct a feasible solution (denoted as φ_{AoI-L}) with its n, f, z, μ and U values kept the same as those in φ_{AoI}^{*} of $G(\mu)$ and $G_2(U)$. Denoting the objective value of the solution φ_{AoI-L} as A_{ave}^{L}, we have:

$$\begin{aligned}
A_{ave}^{L} - A_{ave}^{O*} &= \frac{d}{2}\sum_{l\in\mathcal{L}} G_2(U^{l^*}) + d\sum_{i\in\mathcal{N}}\sum_{j\in\mathcal{T}_i, z_{ij}=1} G(\mu_{ij}^{*}) \\
&\quad - \frac{d}{2}\sum_{l\in\mathcal{L}} g(U^{l^*}) - d\sum_{i\in\mathcal{N}}\sum_{j\in\mathcal{T}_i, z_{ij}=1} g(\mu_{ij}^{*}) \\
&\leq \frac{d}{2}\sum_{l\in\mathcal{L}}\eta_2 + d\sum_{i\in\mathcal{N}}\sum_{j\in\mathcal{T}_i, z_{ij}=1}\eta \ ,
\end{aligned}$$

where the last inequality is derived from Lemma 3. Let $\epsilon = \frac{d}{2}\sum_{l\in\mathcal{L}}\eta_2 + d\sum_{i\in\mathcal{N}}\sum_{j\in\mathcal{T}_i}^{z_{ij}=1}\eta$ and φ_{AoI-L}^{*} denote the optimal solution of OPT-L, with the objective value of A_{ave}^{L*}. Since A_{ave}^{L} is the value of a feasible solution to OPT-L, we have $A_{ave}^{L*} \leq A_{ave}^{L}$. As a result, $A_{ave}^{L*} - A_{ave}^{O*} \leq A_{ave}^{L} - A_{ave}^{O*} \leq \epsilon$. □

Note that (30), (9), and (18) of OPT-L also include the non-linear terms. Those terms can either be reformulated through Reformulation Linearization Technique (RLT) [20], [21], or be automatically linearized by using the boolean expression in the CPLEX solver with great efficiency.

Our complete solution for OPT-AoI is summarized as follows: for a pre-defined approximate error ϵ, we first can calculate the linearization errors η and η_2 and then construct a set of linear segments based on Algorithm 2. After that we reformulate OPT-AoI into OPT-L, which is solved by CPLEX.

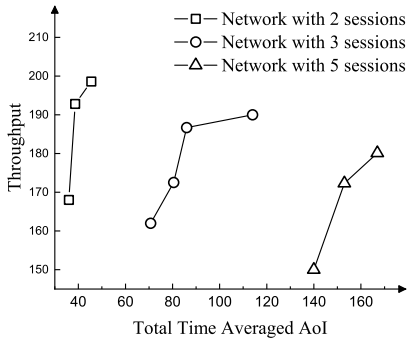

Fig. 3. The AoI and throughput tradeoff with different number of sessions.

V. Numerical Results

In this section, we present the numerical results of AoI and throughput performance in multi-hop networks with flexible routing paths, revealing the achievable AoI and throughput curves under different network settings in multi-hop networks. We randomly generate a 25-node network in a 100×100 area. For generality, we normalize the units for distance, bandwidth, power, packet generation, and transmission rate with appropriate dimensions.

A. Impact of Session Amounts

We increase the number of sessions to 2, 3, and 5. Figure 3 shows the optimal throughput and AoI curves (by connecting all Pareto-optimal points) under different numbers of sessions. From this figure, optimal AoI is seen to drop with an increase in the maximum throughput value. This demonstrates the importance of exploring AoI and throughput relationships when studying AoI in the network. In addition, both AoI and throughput deteriorate as the session count in the networks rises. The reason is that more sessions occupy more network resources, and thus suffering from higher interference in the network. The resource allocated to each session drops, thereby resulting in larger AoI and lower throughput.

B. Impact of Interference Strength

The impact of the interference range on the AoI-throughput curve is unveiled. We randomly generate 3 sessions and vary the interference range from 50, 60, to 70, with AoI-throughput curves depicted in Figure 4. It is seen that both AoI and throughput deteriorate with an increase in the interference range, as expected because a larger interference range results in a lower average activation frequency among links. Thus, throughput drops as the result of a lower bottleneck link

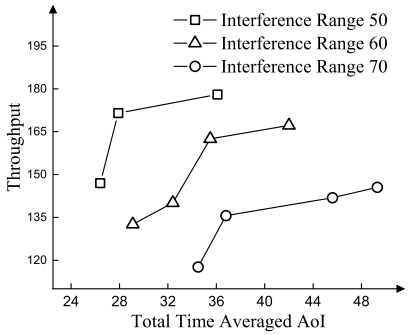

Fig. 4. The AoI and throughput tradeoff with different interference ranges.

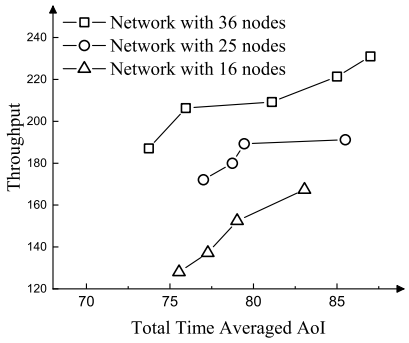

Fig. 5. The AoI and throughput tradeoff with different node density.

transmission rate, and AoI rises with a longer transmission time.

C. Impact of Network Topology

As the network topology changes when the node count rises, we explore the impact of network topology on AoI and throughput tradeoffs by varying the number of nodes from 16, 25, to 36 in the 100×100 area. In each setting, 3 sessions are randomly generated. Figure 5 shows the Pareto-optimal curves between throughput and AoI under different numbers of nodes in the network. We can observe that as the number of nodes increases, the throughput increases significantly while AoI exhibits moderate trends in its value changes. The reason is that, with increased nodes density, the average transmission distance of each activated link in all sessions decreases, thereby heightening the averaged link capacity to improve the network throughput. On the other hand, the optimal AoI prefers routes with fewer nodes, and hence higher node density only lifts the choice of link selection for AoI optimization and fails to improve this metric significantly.

Moreover, when the throughput reaches the maximum value, AoI becomes a little bit worse with further more nodes in the network than without. For a multi-hop network with more nodes, its throughput is improved with more relay nodes to shorten the bottleneck link, resulting in higher interference among the increased number of links to damage the average transmission rate and AoI.

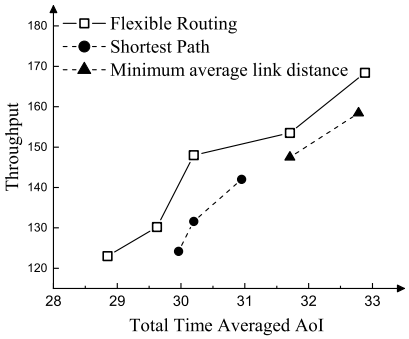

Fig. 6. The AoI and throughput tradeoff under different routing schemes.

D. Comparison with Different Routing Schemes

We now fix the number of nodes as 25 and generate a single session to explore the impact of routing selection on our solution. As there does not exist solutions exploring the routing and AoI-throughput tradeoff in multi-hop networks, we take the shortest path and the minimum averaged link distance schemes into consideration for comparison, with the results depicted in Figure 6. By comparing three Pareto-optimal curves, we can see our flexible routing solution achieves the best in both throughput and AoI. This demonstrates the advantage of our proposed flexible routing scheme. Meanwhile, the shortest path scheme exhibits better AoI while the minimum averaged link distance scheme enjoys higher network throughput, when comparing two of them. The reason is that the shortest path scheme involves fewer relay nodes to yield less transmission delay, thus the larger average transmission rate leading to lower AoI. The minimum averaged link distance scheme can result in larger bottleneck link capacity, which helps to lift the throughput. On the other hand, more relay nodes involved in this scheme heighten AoI.

VI. Conclusion

This paper has presented an in-depth study on the optimal AoI and throughput tradeoff in multi-hop networks for the first time, with such physical factors as channel allocation, scheduling, and flexible routing selection taken into consideration. A rigorous mathematical model is developed to characterize the interrelation of AoI and throughput. By formulating a multi-objective problem and developing a novel algorithm to find Pareto-optimal points, we identify all tradeoff points of the optimal AoI and throughput. Our algorithm has been proved to find all Pareto-optimal points with a finite number of iterations. The simulation results demonstrate the existence of a tradeoff between AoI and throughput, with one performance metric to improve while degrading the other metric. Our mathematical development, algorithmic solutions, and results included in this paper shed light on wireless network design by relating two key performance metrics, calling for AoI and throughput optimization simultaneously, instead of optimizing one single metric individually.

ACKNOWLEDGMENTS

This work was supported in part by Louisiana Board of Regents under Contract Numbers LEQSF(2018-21)-RD-A-24 and in part by NSF under Grants 1652107 and 1763620.

REFERENCES

[1] S. Kaul, R. Yates, and M. Gruteser, "Real-time status: How often should one update?" in *Proceedings of IEEE International Conference on Computer Communications (INFOCOM)*, 2012, pp. 2731–2735.

[2] R. D. Yates and S. Kaul, "Real-time status updating: Multiple sources," in *Proceedings of IEEE International Symposium on Information Theory (ISIT)*, 2012, pp. 2666–2670.

[3] Y. Sun, E. Uysal-Biyikoglu, R. Yates, C. E. Koksal, and N. B. Shroff, "Update or wait: How to keep your data fresh," in *Proceedings of IEEE International Conference on Computer Communications (INFOCOM)*, 2016, pp. 1–9.

[4] M. Costa, M. Codreanu, and A. Ephremides, "Age of information with packet management," in *Proceedings of IEEE International Symposium on Information Theory (ISIT)*, 2014, pp. 1583–1587.

[5] ——, "On the age of information in status update systems with packet management," *IEEE Transactions on Information Theory*, vol. 62, no. 4, pp. 1897–1910, 2016.

[6] N. Pappas, J. Gunnarsson, L. Kratz, M. Kountouris, and V. Angelakis, "Age of information of multiple sources with queue management," in *Proceedings of IEEE International Conference on Communications (ICC)*, 2015, pp. 5935–5940.

[7] S. K. Kaul, R. D. Yates, and M. Gruteser, "Status updates through queues," in *Proceedings of Annual Conference on Information Sciences and Systems (CISS)*, 2012, pp. 1–6.

[8] A. M. Bedewy, Y. Sun, and N. B. Shroff, "Optimizing data freshness, throughput, and delay in multi-server information-update systems," in *Proceedings of IEEE International Symposium on Information Theory (ISIT)*, 2016, pp. 2569–2573.

[9] ——, "Minimizing the age of the information through queues," 2017. [Online]. Available: https://arxiv.org/abs/1709.04956

[10] Y. Sun, E. Uysal-Biyikoglu, and S. Kompella, "Age-optimal updates of multiple information flows," 2018. [Online]. Available: https://arxiv.org/abs/1801.02394

[11] R. D. Yates and S. K. Kaul, "Status updates over unreliable multiaccess channels," in *Proceedings of IEEE International Symposium on Information Theory (ISIT)*, 2017, pp. 331–335.

[12] Z. Jiang, B. Krishnamachari, X. Zheng, S. Zhou, and Z. Niu, "Decentralized status update for age-of-information optimization in wireless multiaccess channels," in *Proceedings of IEEE International Symposium on Information Theory (ISIT)*, 2018, pp. 2276–2280.

[13] R. Talak, S. Karaman, and E. Modiano, "Optimizing information freshness in wireless networks under general interference constraints," in *Proceedings of ACM International Symposium on Mobile Ad Hoc Networking and Computing (MobiHoc)*, 2018, pp. 61–70.

[14] I. Kadota, A. Sinha, and E. Modiano, "Optimizing age of information in wireless networks with throughput constraints," in *Proceedings of IEEE International Conference on Computer Communications (INFOCOM)*, 2018, pp. 1844–1852.

[15] R. D. Yates, "Lazy is timely: Status updates by an energy harvesting source," in *Proceedings of IEEE International Symposium on Information Theory (ISIT)*, 2015, pp. 3008–3012.

[16] I. Kadota, E. Uysal-Biyikoglu, R. Singh, and E. Modiano, "Minimizing the age of information in broadcast wireless networks," in *IEEE Annual Allerton Conference on Communication, Control, and Computing (Allerton)*, 2016, pp. 844–851.

[17] J. Selen, Y. Nazarathy, L. L. H. Andrew, and L. V. Hai, "The age of information in gossip networks," *Environmental Technology*, vol. 27, no. 8, pp. 863–873, 2013.

[18] A. Arafa and S. Ulukus, "Age-minimal transmission in energy harvesting two-hop networks," in *Proceedings of IEEE Global Communications Conference (GLOBECOM)*, 2017, pp. 1–6.

[19] R. Talak, S. Karaman, and E. Modiano, "Minimizing age-of-information in multi-hop wireless networks," in *Proceedings of Allerton Conference on Communication, Control, and Computing (Allerton)*, 2017, pp. 486–493.

[20] H. D. Sherali and W. P. Adams, *A reformulation-linearization technique for solving discrete and continuous nonconvex problems, Chapter 8*. Kluwer Academic Publishers, 1999.

[21] Y. T. Hou, Y. Shi, and H. D. Sherali, *Applied optimization methods for wireless networks*. Cambridge University Press, 2014.